A MODEL OF COMPRESSIBLE JET PENETRATION

W. J. Flis
DE Technologies, Inc., 100 Queens Drive, King of Prussia, PA, 19406, U.S.A.

Recently [1], a model of compressible jet penetration was developed that is self-consistent in that the same Hugoniot relation, a linear dependence of shock velocity on particle velocity, was used both to describe the conditions across the shock that occurs in each material at supersonic velocities and to derive the Mie-Grüneisen equation of state of each material. This model is extended to a quadratic dependence of shock velocity on particle velocity and to a specific heat that varies with temperature and volume. Model predictions with and without accounting for the presence of shocks are compared with the classical incompressible model. Hydrocode computations provide some support for the compressible model.

INTRODUCTION

Previous models of compressible jet penetration differed mainly in the choices made for the equation of state (EOS). All, however, relied on the same form of the Hugoniot relation, a linear dependence of shock velocity U_s on particle velocity U_p,

$$U_s = C_0 + S_1 U_p \tag{1}$$

For the EOS, Haugstad [2], Haugstad and Dullum [3], and Federov and Bayanova [4] all adopted forms of Murnaghan's relation,

$$1 + \beta(4b-1)(p - p_1) = \left(\frac{v_1}{v}\right)^{4b-1}$$

Flis and Chou [5] used a Mie-Grüneisen EOS of the form

$$p = \left(k_1\mu + k_2\mu^2 + k_3\mu^3\right)\left(1 - \frac{\Gamma\mu}{2}\right) + \frac{\Gamma}{v}\left(E - E_0\right)$$

which, depending on the parameter values, is not necessarily consistent with Eq. (1).

Osipenko and Simonov [1] derived a self-consistent model of compressible jet penetration by using a Mie-Grüneisen EOS derived from Eq. (1),

$$p = \frac{\rho_0 C_0^2 \eta}{\left(1 - S_1\eta\right)^2}\left(1 - \frac{\Gamma\mu}{2}\right) + \frac{\Gamma}{v}\left(E - E_0\right) \tag{2}$$

In the present paper, a quadratic counterpart of Eq. (1) is combined with a form of the Mie-Grüneisen EOS that is entirely consistent with it.

Also, previous models that included a solution for temperatures assumed a constant specific heat. In this paper, the specific heat is assumed to vary with volume and temperature according to the Debye theory, but the result of incorporating this is shown to be small.

PRESENT MODEL

In this paper, the quadratic Hugoniot relation

$$U_s = C_0 + S_1 U_p + \frac{S_2}{C_0} U_p^2 \tag{3}$$

is adopted instead of Eq. (1). This is used with the Mie-Grüneisen EOS,

$$E(p,v) = E_h + \frac{p - p_h}{\rho\Gamma} \tag{4}$$

where E is internal energy, p is pressure, $v = 1/\rho$ is specific volume, and $\Gamma \equiv v(\partial p / \partial E)_v$ is the Grüneisen parameter. Energy and pressure along the Hugoniot are given as functions of volume by

$$E_h = \frac{\eta p_h}{2\rho_0} \tag{5}$$

$$p_h = \begin{cases} \dfrac{\rho_0 C_0^2 \eta}{(1 - S_1\eta)^2}, & \text{for } S_2 = 0 \\ \dfrac{\rho_0 C_0^2}{4\eta^3 S_2^2}\left[1 - S_1\eta - \sqrt{(1 - S_1\eta)^2 - 4S_2\eta^2}\right]^2, & \text{for } S_2 \neq 0 \end{cases} \tag{6}$$

where $\eta \equiv (v_0 - v)/v_0$. Note that Eq. (6) is derived from Eq. (3) and the Rankine-Hugoniot relations. It is assumed that Γ is independent of pressure and is given by the relation $\rho\Gamma = \rho_0\Gamma_0$.

To analyze the penetration process, the flow is visualized in a coordinate system moving with the penetration zone, that is, at the penetration velocity U, as shown in Fig. 1. Then the point on the centerline at the interface between the jet and target is a stagnation point in the flow. Let W denote flow velocity relative to and toward the stagnation point. The boundary conditions at infinity are, in the target,

$$W_{0t} = U; \quad p_{0t} = 0; \quad E_{0t} = 0 \tag{7}$$

and, in the jet,

$$W_{0j} = V - U; \quad p_{0j} = 0; \quad E_{0j} = 0 \tag{8}$$

If the flow in either material relative to its stagnation point is supersonic ($W_0 > C_0$), then a shock will stand at some distance from the stagnation point. Conditions across the shock at states 0 and 1 are related by the Rankine-Hugoniot equations,

$$\rho_0 W_0 = \rho_1 W_1 \tag{9}$$

$$p_0 + \rho_0 W_0^2 = p_1 + \rho_1 W_1^2 \tag{10}$$

$$p_0 v_0 + \tfrac{1}{2} W_0^2 + E_0 = p_1 v_1 + \tfrac{1}{2} W_1^2 + E_1 \tag{11}$$

The velocity of the shock relative to the material ahead of it is $U_s = W_0$, and the flow velocity behind the shock is $W_1 = U_s - U_p$. Thus, by Eq. (3),

$$W_1 = \begin{cases} W_0 - (W_0 - C_0)/S_1 & \text{for } S_2 = 0 \\ W_0 - C_0\left(S_1 - \sqrt{S_1^2 + 4S_2(W_0 - C_0)/C_0}\right)/2S_2 & \text{for } S_2 \neq 0 \end{cases} \tag{12}$$

By Eqs. (9-11), the remaining conditions behind the shock are given by

$$\rho_1 = \rho_0 W_0 / W_1 \tag{13}$$

$$p_1 = p_0 + \rho_0 W_0^2 - \rho_0 W_0 W_1 \tag{14}$$

$$E_1 = p_0 v_0 + \tfrac{1}{2} W_0^2 + E_0 - p_1 v_1 - \tfrac{1}{2} W_1^2 \tag{15}$$

Given the conditions at state 0, those at state 1 are known from Eqs. (12-15).

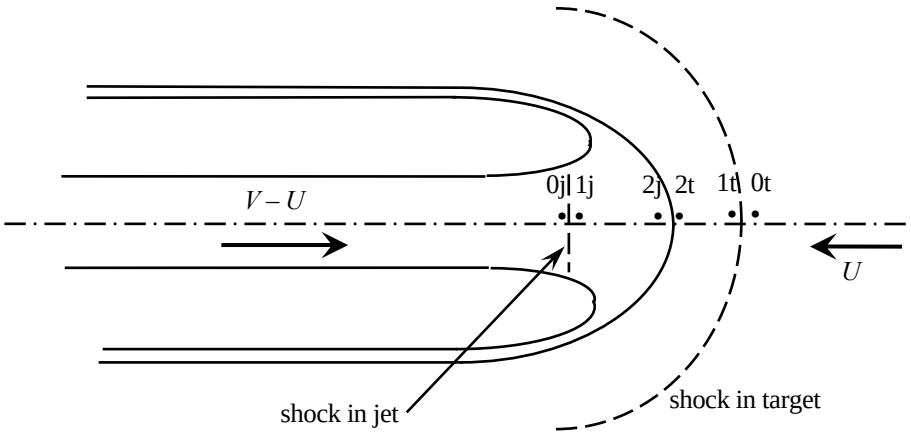

Figure 1. Flow field in moving coordinates and flow stations.

Conditions at states 1 and 2 are related by the compressible Bernoulli equation,

$$p_1 v_1 + \tfrac{1}{2} W_1^2 + E_1 = p_2 v_2 + \tfrac{1}{2} W_2^2 + E_2 \tag{16}$$

where the internal energies are related by the isentropic relation,

$$E_2 - E_1 = -\int_1^2 p\,dv \tag{17}$$

in which the integral is taken along the isentrope. If there is no shock, Eqs. (9-11) are not used, and Eqs. (16-17) are applied between states 0 and 2.

Now, at any point x along the streamline from state 1, the compressible Bernoulli's equation,

$$p_1 v_1 + \tfrac{1}{2} W_1^2 = p_x v_x + \tfrac{1}{2} W_x^2 + \int_1^x p\,dv \tag{18}$$

must hold. To find state 2, this equation is rearranged to

$$\tfrac{1}{2} W_x^2 = p_x v_x + \int_1^x p\,dv - p_1 v_1 - \tfrac{1}{2} W_1^2 \tag{19}$$

which is integrated numerically from state 1 in a direction of decreasing volume v until $\tfrac{1}{2} W_x^2 = 0$, since state 2 in each material is a stagnation point, where $W_2 = 0$.

A last condition requires equilibrium across the interface between the stagnation points, $p_{2j} = p_{2t}$. To apply this, Eqs. (11) and (16) are combined to

$$p_2 v_2 + \tfrac{1}{2} W_2^2 + E_2 = p_0 v_0 + \tfrac{1}{2} W_0^2 + E_0 \tag{20}$$

Since $W_2 = 0$ in both jet and target, this equation may be solved for p_2,

$$p_2 = \left(\tfrac{1}{2} W_0^2 + p_0 v_0 - E_2 + E_0\right) / v_2 \tag{21}$$

Applying this in the target, where $W_{0t} = U$, and in the jet, where $W_{0j} = V - U$, and equating stagnation pressures yields

$$\tfrac{1}{2}(V-U)^2 + p_{0j} v_{0j} - E_{2j} + E_{0j} = \frac{v_{2j}}{v_{2t}}\left(\tfrac{1}{2} U^2 + p_{0t} v_{0t} - E_{2t} + E_{0t}\right) \tag{22}$$

which, defining $\phi \equiv \left(v_{0t} v_{2j}\right) / \left(v_{0j} v_{2t}\right)$, may be rearranged to

$$\left(\frac{V-U}{U}\right)^2 = \frac{\rho_{0t}}{\rho_{0j}}\left[\phi + \frac{\phi p_{0t} - p_{0j} - \phi\left(E_{2t} - E_{0t}\right)\rho_{0t} + \left(E_{2j} - E_{0j}\right)\rho_{0j}}{\tfrac{1}{2}\rho_{0t} U^2}\right] \tag{23}$$

For a given V, this system of equations is solved by the method of successive substitution, as in [2]. Using an assumed value of U, the right-hand side of Eq. (23) is evaluated, from which a new value of U is found. That is, if Eq. (23) is written as

$$\left(\frac{V-U}{U}\right)^2 = \frac{\rho_{0t}}{\rho_{0j}} \psi^{-1} \tag{24}$$

then the updated value of U is

$$U = \frac{V}{1 + \sqrt{\frac{\rho_{0t}}{\rho_{0j}} \psi^{-1}}} \tag{25}$$

where ψ is computed from the previous value of U. Updating U is repeated until convergence.

Comparison with Incompressible Theory

The penetration P per unit length L of jet is

$$dP / dL = U / (V - U) \tag{26}$$

By Eq. (24), this is

$$dP / dL = \sqrt{(\rho_{0j} / \rho_{0t}) \psi} \tag{27}$$

while, according to the incompressible theory of jet penetration,

$$dP / dL = \sqrt{\rho_{0j} / \rho_{0t}} \tag{28}$$

Thus, the ratio of compressible to incompressible penetration per unit jet length is (as in [2])

$$\frac{P_{compressible}}{P_{incompressible}} = \sqrt{\psi} \tag{29}$$

Temperature

The equations above determine the pressure, volume, flow velocity, and energy at the key stations of the flow. Determination of temperatures requires additional equations.

Haugstad and Dullum [3] estimated the temperature behind the shock using weak shock theory. To perform the same estimation, Osipenko and Simonov [1] numerically integrated a thermodynamic identity along the Hugoniot, using a constant specific heat c_v. Both then used an exact integral along the isentrope to find the temperature at the stagnation point. The method of [1] is adopted here, except that c_v is taken as a function of absolute temperature T and volume given by Debye theory.

The temperature just behind each shock may be calculated by means of the identity

$$\frac{dT}{T} = -\Gamma \frac{dv}{v} + \frac{ds}{c_v} \tag{30}$$

Combining this with the first law, $dE = Tds - pdv$, and taking derivatives along the Hugoniot yields

$$c_v(T,v)\frac{dT_h(v)}{dv} + \frac{\Gamma c_v(T,v)}{v}T_h(v) = \frac{dE_h(v)}{dv} + p_h(v) \tag{31}$$

where the Hugoniot energy and pressure are given by Eqs. (5-6). By Eq. (5),

$$\frac{dT_h}{dv} + \frac{\Gamma}{v}T_h = \frac{1}{2c_v}\left[\frac{\eta}{\rho_0}\frac{dp_h}{dv} + p_h\right] \tag{32}$$

as given in [1]. Performing the differentiations using Eq. (6) yields

$$\frac{dT_h}{dv} + \frac{\Gamma}{v}T_h = \begin{cases} -\dfrac{\rho_0 C_0^2}{c_V}\dfrac{S_1\eta^2}{(1-S_1\eta)^3} & \text{for } S_2 = 0 \\ \dfrac{1}{c_v}\left[2p_h + \dfrac{\rho_0 C_0^2}{8\eta^2 S_2^2}\left(S_1 - \dfrac{(1-S_1\eta)S_1 + 4S_2\eta}{\sqrt{(1-S_1\eta)^2 - 4S_2\eta^2}}\right)\times\right. & \text{for } S_2 \neq 0 \\ \left.\times\left(1 - S_1\eta - \sqrt{(1-S_1\eta)^2 - 4S_2\eta^2}\right)\right] & \end{cases} \tag{33}$$

which, given expressions for the specific heat and Grüneisen parameter, may be integrated numerically. (This result for the case $S_2 = 0$ is given in [1].) The specific heat is given by Debye theory [6] as

$$c_v(T,v) = 3nk\left[4D_3\left(\theta(v)/T\right) - 3\frac{\theta(v)/T}{\exp\left[\theta(v)/T\right] - 1}\right] \tag{34}$$

where n is the number of atoms, k is the Boltzmann constant, D_3 is the third Debye function, $D_3(x) = \dfrac{3}{x^3}\int_0^x \dfrac{t^3}{e^t - 1}dt$, and θ is the Debye temperature,

$$\theta(v) = \theta_0 \exp\int_v^{v_0}\frac{\Gamma}{v}dv \tag{35}$$

Again assuming $\rho\Gamma = \rho_0\Gamma_0$, this may be integrated to

$$\theta(v) = \theta_0 \exp\left[\Gamma_0\left(1 - v/v_0\right)\right] \tag{36}$$

Values of initial Debye temperature θ_0 for several materials are given by Kinslow [7]. If θ_0 is unknown, Eq. (34) may be solved to determine it from c_{v0}, the specific heat at standard conditions.

With Eqs. (34-36), Eq. (33) may be integrated from the initial state along the Hugoniot to the conditions at station 1. Using the integrating factor $\exp\left(\Gamma_0 v/v_0\right)$ yields

$$T_h \exp\left(\frac{\Gamma_0 v_h}{v_0}\right) = T_0 \exp(\Gamma_0) + \int_{v_0}^{v_h} F(v, T_h) \exp\left(\frac{\Gamma_0 v}{v_0}\right) dv \tag{37}$$

where $F(v, T)$ is the right-hand side of Eq. (33). This is integrated numerically along the Hugoniot until the volume v_1 is reached.

To find the temperature at the stagnation point, we follow previous papers by noting that the flow between stations 1 and 2 is adiabatic, $ds = 0$, which neglects heat conduction and the contribution of plastic work. Then Eq. (30) reduces to

$$\frac{dT}{T} = -\frac{\Gamma}{v} dv \tag{38}$$

the integral of which between these stations is

$$T_2 = T_1 \exp\left(\Gamma_0 \frac{v_1 - v_2}{v_0}\right) \tag{39}$$

CALCULATED RESULTS

The model was exercised for a copper jet penetrating polymethyl methacrylate (PMMA, Plexiglas) using material properties in Table I. The results are shown in Fig. 2, a plot of penetration per unit length of jet relative to the incompressible theory versus jet velocity. Two curves are shown, one accounting for the presence of the shocks and the other not; the curves coincide up to a jet velocity of about 3.6 km/s, when a shock begins to occur in the target.

This result shows that accounting for the shock in the target yields a larger penetration than when the shock is not accounted for. This may be understood by recognizing that the p-v Hugoniot curve of any material is stiffer (i.e., less compressible) than its isentrope, so that accounting for the shock makes the target seem less compressible, and hence reduces the effect of compressibility on reducing penetration. This trend is opposite that predicted by the models of [3] and [5], which showed a greater effect of compressibility when shocks are accounted for.

Table I. Material properties.

	Copper	*Steel*	*PMMA*
Initial mass density, ρ_0 (Mg/m^3)	8.93	7.85	1.186
Bulk sound speed, C_0 (km/s)	3.940	3.574	2.300
Hugoniot parameter, S_1	1.489	1.92	1.750
Hugoniot parameter, S_2	0.0	–0.068	–0.013
Grüneisen coefficient, Γ_0	1.99	1.69	0.91
Initial Debye temperature θ_0 (K)	306	175	266

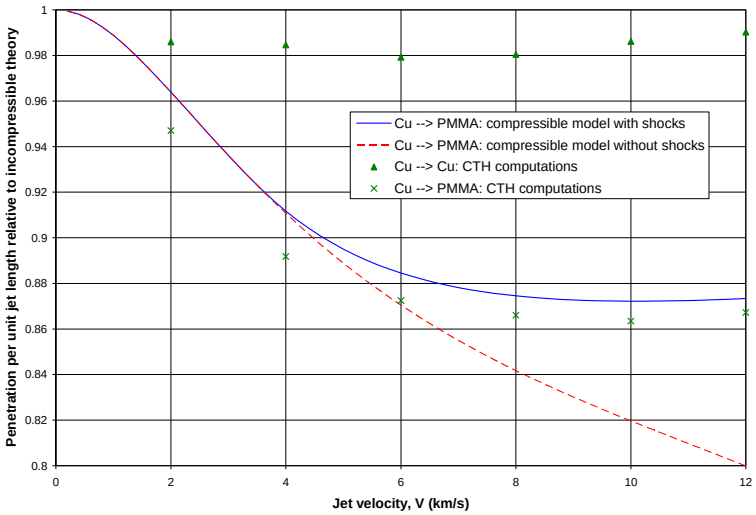

Figure 2. Ratio of penetrations according to the compressible and incompressible models vs. jet velocity for a copper jet penetrating PMMA, with and without accounting for the presence of shocks in the compressible model.

Comparison with Hydrocode Computations

CTH code computations were performed to compare with the model. A 4-mm-radius copper jet impacts a semi-infinite target at velocities of 2, 4, … 12 km/s. All strength properties were set to zero. A 0.25-mm mesh was used. Results were analyzed by the following method: when the penetration zone reached a depth of about 64 mm, the time and actual penetration depth (read from material plot) were recorded; this was repeated at about 196 mm of penetration. From these data, the penetration velocity U was computed. Then the penetration per unit jet length dP/dL was computed by Eq. (26) and compared with the incompressible-theory value, Eq. (28).

Figure 2 includes data for targets of copper and PMMA. For a copper jet impacting a copper target, the compressible and incompressible theories predict the same penetration velocity, equal to half the jet velocity; thus, the ratio between the two theories is unity. However, the corresponding CTH data points fall 1% to 2% below that value, which may be attributed to the simulation having not quite yet reached a steady state (penetration velocity was observed to be increasing very slowly).

For the PMMA target, the data approximately follow the compressible model curve (with shocks), falling below it by about the same small amount as the copper-target data fall below unity. This provides some verification of the present model.

Computed Temperatures

Some computations using the model indicate the highest temperatures in the jet and target, which are reached at the stagnation points. Previous studies [8,9] have indicated that the external temperature of a typical copper shaped-charge jet shortly after formation is about 697°K. If a jet at this temperature impacts a steel target at 10 km/s, its stagnation temperature is predicted to be 1376°K (not accounting for phase change), slightly above copper's melt temperature of 1357°K. There is, however, no melting in the steel even at this velocity, as its temperature reaches only 713°K, whereas its melt temperature is 1808°K.

Effect of Non-constant Specific Heat

In the model, the dynamical equations used for computing the penetration velocity are independent of the thermodynamic equations used to compute temperature; therefore, the specific heat can have no effect on penetration velocity. However, the specific heat and its dependence on state variables of course does affect computed temperatures.

The temperature and volume dependence of the specific heat, given by Eqs. (34) and (36), is only weak. Indeed, it is easily shown from these equations that, along any isentrope, c_v is constant (because the ratio θ/T is constant there), so unless a shock is present, c_v will be constant. Calculations with the model show, for example, that for a 10-km/s copper jet penetrating PMMA (which may be considered an extreme case), the Debye theory predicts a stagnation temperature of 2096°K, while a constant specific heat yields 2148°K, only slightly different.

CONCLUSIONS

A self-consistent model of the effect of compressibility on jet penetration previously derived by Osipenko and Simonov has been extended and exercised. A quadratic form of the shock-velocity–particle-velocity Hugoniot curve and a non-constant specific heat have been substituted. The effect of accounting for the existence of a shock wave in the target is shown by this model to decrease the effect of compressibility, a trend opposite that shown in previous work. Also, the effect of considering a non-constant value of specific heat is shown to be small, which supports the assumption of a constant value of specific heat. Finally, comparisons with hydrocode computations support the validity of the model.

REFERENCES

1. K.Yu. Osipenko and I.V. Simonov, 2009, "On the jet collision: general model and reduction to the Mie–Grüneisen state equation," *Izvestiya Akademii Nauk. Mekhanika Tverdogo Tela*, no. 4, 172-182; also, *Mech. Solids*, 44(4):639–648.
2. B.S. Haugstad, 1981, "Compressibility effects in shaped charge jet penetration," *J. Appl. Phys.*, 52(3):1243–1246.
3. B.S. Haugstad and O.S. Dullum, 1981, "Finite compressibility in shaped charge jet and long rod penetration—the effect of shocks," *J. Appl. Phys.*, 52(8):5066–5071.
4. S.V. Federov and Ya.M. Bayanova, 2010, "Hydrodynamic model for penetration of extended projectiles with consideration of material compressibility," *Proc. 25th Inter. Symp. Ballistics*, Beijing, China, 17–21 May.
5. W.J. Flis and P.C. Chou, 1983, "Penetration of compressible materials by shaped-charge jets," *Proc. 7th Inter. Symp. Ballistics*, The Hague, The Netherlands, 19–21 April.
6. V.N. Zharkov and V.A. Kalinin, 1971, *Equations of State for Solids at High Pressures and Temperatures*, Albin Tybulewicz, trans., Consultants Bureau, N.Y.
7. R. Kinslow (ed.), 1970, *High-Velocity Impact Phenomena*, Academic Press, N.Y.
8. W.G. von Holle and J.J. Trimble, 1976, "Temperature measurement of shocked copper plates and shaped charge jets by two-color IR radiometry," *J. Appl. Phys*., 47(6):2391–2394.
9. W.G. von Holle and J.J. Trimble, 1976, "Shaped charge temperature measurement," *Sixth Symp. (Intl.) Detonation*, San Diego, 24–27 Aug.